Kandidaatintutkielma
Fysikaalisten tieteiden kandiohjelma
Teoreettinen fysiikka

Detection of primordial black holes with LISA

Santeri Rusanen

June 29, 2026

Supervisor(s): Syksy Räsänen

Examiner(s): Syksy Räsänen

University of Helsinki
Matemaattis-luonnontieteellinen tiedekunta

PL 64 (Gustaf Hällströmin katu 2a)
00014 Helsingin yliopisto

HELSINGIN YLIOPISTO — HELSINGFORS UNIVERSITET — UNIVERSITY OF HELSINKI

Tiedekunta — Fakultet — Faculty	Koulutusohjelma — Utbildningsprogram — Degree programme
Matemaattis-luonnontieteellinen tiedekunta	Fysikaalisten tieteiden kandiohjelma Teoreettinen fysiikka

Tekijä — Författare — Author

Santeri Rusanen

Työn nimi — Arbetets titel — Title

Detection of primordial black holes with LISA

Työn laji — Arbetets art — Level	Aika — Datum — Month and year	Sivumäärä — Sidantal — Number of pages
Kandidaatintutkielma	June 29, 2026	19

Tiivistelmä — Referat — Abstract

If the comoving curvature power spectrum is enhanced strongly enough at small scales, the resulting induced gravitational wave background is detectable, and some fluctuations can collapse into primordial black holes. The induced gravitational waves are the second-order tensor perturbations generated by the terms that are quadratic in the first-order perturbations.

First, we go over the criterion for primordial black hole formation and constraints on their abundance. We then expand the perturbed Einstein equations to second order, derive the equation of motion of the gravitational waves, and calculate their energy density. We show that if primordial black holes make up a significant portion of dark matter, the signal will be detected by the Laser Interferometer Space Antenna (LISA) for a monochromatic enhancement of the comoving curvature spectrum, and explain how the signal changes for other spectra. After that, we discuss the sensitivity of LISA, other space-based detectors, and the implications of a detection or non-detection for primordial black hole dark matter.

Avainsanat — Nyckelord — Keywords

Säilytyspaikka — Förvaringsställe — Where deposited

Muita tietoja — Övriga uppgifter — Additional information

Tiedekunta — Fakultet — Faculty
Matemaattis-luonnontieteellinen tiedekunta

Koulutusohjelma — Utbildningsprogram — Degree programme
Fysikaalisten tieteiden kandiohjelma
Teoreettinen fysiikka

Tekijä — Författare — Author
Santeri Rusanen

Työn nimi — Arbetets titel — Title
Detection of primordial black holes with LISA

Työn laji — Arbetets art — Level	Aika — Datum — Month and year	Sivumäärä — Sidantal — Number of pages
Kandidaatintutkielma	June 29, 2026	19

Tiivistelmä — Referat — Abstract

Jos universumin tiheysvaihtelut ovat riittävän suuria pienillä skaaloilla, ne aiheuttavat gravitaatioaaltotaustan, ja osa niistä voi romahtaa muinaisiksi (primordiaalisiksi) mustiksi aukoiksi. Nämä indusoidut gravitaatioaallot ovat toisen kertaluvun tensoriperturbaatioita, jotka syntyvät ensimmäisen kertaluvun skalaariperturbaatioiden kvadraattisista termeistä.

Aluksi käymme läpi muinaisten mustien aukkojen muodostumiskriteerit ja havaintojen asettamia rajoituksia niiden määrälle. Sitten käytämme toisen kertaluvun perturboituja Einsteinin yhtälöitä ja johdamme gravitaatioaaltojen liikeyhtälön ja laskemme niiden energiatiheyden. Osoitamme, että jos huomattava osa pimeästä aineesta koostuu muinaisista mustista aukoista, monokromaattisia tiheysvaihteluja vastaava gravitaatioaaltosignaali on havaittavissa Laser Interferometer Space Antenna (LISA)-detektorilla. Seuraavaksi käsittelemme miten signaali muuttuu erilaiselle tiheysvaihtelujen tehospektrille. Tämän jälkeen keskustelemme LISAn herkkyydestä, muista detektoreista ja siitä, mitä signaalin havaitseminen tai sen puute kertoo primordiaalisten mustien aukkojen määrästä.

Avainsanat — Nyckelord — Keywords

Säilytyspaikka — Förvaringsställe — Where deposited

Muita tietoja — Övriga uppgifter — Additional information

Contents

1. Introduction

Black holes are regions of spacetime inside which gravitation is so strong even light can't exit. In addition to astrophysical black holes formed from stellar evolution, there exists the possibility of primordial black holes (PBHs) which could be produced in the early universe [1]. There are many ways for PBHs to form, but we shall focus on the most popular candidate, the collapse of density fluctuations caused by inflation. The inflationary scenario introduces a period of accelerated expansion in the early universe that explains the statistical homogeneity, isotropy and the apparent spatial flatness of the universe, while also predicting the observed perturbations. During inflation, the energy density of the universe is dominated by the inflaton field whose potential energy is much larger than its kinetic energy [2]. As the universe expands, the quantum fluctuations of the field also stretch to cosmological lengths. The amplitude of the perturbations on large scales has been measured from the cosmic microwave background (CMB) to be around 10^{-5}, but some models of inflation produce stronger perturbations on smaller scales [3]. A significant number of PBHs could be generated if the amplitude of the fluctuations on small scales was 10^4 times greater than the one observed on the CMB scales. The perturbations on larger scales act as seeds for galaxies and other structures, while on smaller scales they can in rare cases collapse to PBHs.

A significant amount of PBHs could explain many observations. One of the biggest questions in cosmology is what dark matter is. In the 1970s there started to be convincing evidence from the rotation curves of galaxies that much of the mass inside them is not visible and lies outside the optical edge of the galaxy [4]. Today it's believed that around 85% of matter in the universe is made of cold non-baryonic dark matter [1]. PBHs are a possible candidate for dark matter, since they form in the early universe and are stable if their masses are large enough, since Hawking radiation weakens as the black hole mass increases. Other observations PBHs could also explain are gravitational wave signals from binaries with unexpected masses. The LIGO/Virgo/KAGRA collaboration has observed black hole mergers with masses that might be in the intermediate ($10^2 M_\odot < M < 10^4 M_\odot$) or sub solar mass range, that can't form through stellar collapse, though intermediate mass black holes can still be produced by accretion, and there has been only one sub solar mass observation which could be a false positive [5, 6]. There are also observations of

supermassive black holes from when the universe was under 600 million years old, which is earlier than expected but could be explained by PBHs [7].

Only few fluctuations with the largest amplitudes will collapse into PBHs, but as we will show later, all of the fluctuations will contribute to a gravitational wave background that today ranges from a few Hz to nHz. These gravitational waves can't be detected with the current ground based detectors, which have their best sensitivity at ~ 500 Hz [8], but future instruments like the Laser Interferometer Space Antenna (LISA), with a peak sensitivity in the mHz range could detect the signal if the fluctuations were amplified on small scales. In addition to learning about PBHs, a gravitational wave detection would allow us to probe the early universe and the inflation model.

In the second chapter we will go over the formation of PBHs and constraints from observations. In the third chapter we show that the fluctuations induce gravitational waves and calculate their energy density. Finally, in the fourth chapter we compare the energy density to the sensitivity of LISA and discuss what an observation (or lack of one) means. We use natural units, where $c = \hbar = k_B = 1$.

2. Primordial black holes

2.1 Formation of primordial black holes

We can describe the fluctuations using perturbation theory. Considering second-order perturbations around a spatially flat Friedmann–Lemaitre–Robertson–Walker (FLRW) universe, the metric tensor is

$$g_{\alpha\beta} = g^{(0)}_{\alpha\beta} + \delta^{(1)} g_{\alpha\beta} + \delta^{(2)} g_{\alpha\beta} \ , \tag{2.1}$$

where the superscript indicates the order of perturbation and $g^{(0)}_{\alpha\beta}$ is the background metric. Using the longitudinal gauge, we write the perturbed metric as [9]

$$\mathrm{d}s^2 = a^2(\eta) \left[-(1+2\Phi)\mathrm{d}\eta^2 + \left(\{1-2\Psi\}\delta_{ij} + \frac{1}{2} h_{ij} \right) \mathrm{d}x^i \mathrm{d}x^j \right] \ , \tag{2.2}$$

where $a(\eta)$ is the scale factor, η is conformal time, Φ and Ψ are the first order scalar perturbations and h_{ij} are the tensor perturbations. We consider only tensor perturbations at second order $h_{ij} = h^{(2)}_{ij}$, and we have also dropped all vector perturbations since scalar field inflation does not produce them. The fluctuations are described by the comoving curvature perturbation [10]

$$\zeta = -\Psi - \frac{2}{3(1+w)} (\mathcal{H}^{-1}\Psi' + \Phi) \ , \tag{2.3}$$

where w is the equation of state parameter, $\mathcal{H}$ is the conformal Hubble parameter and $' \equiv \frac{\mathrm{d}}{\mathrm{d}\eta}$. A PBH forms if the maximum value of the compaction function $\mathcal{C} = \frac{2G_\mathrm{N}\Delta M}{R}$ is greater than a critical value $\mathcal{C}_\mathrm{th}$, where G_N is the gravitational constant, ΔM is the extra mass compared to the unperturbed universe and R is the areal radius. The gradient expansion allows us to write the compaction function for super-Hubble scales in terms of the comoving curvature perturbation as $\mathcal{C}(r) = \frac{2}{3}\left[1 - (1 + r\frac{\partial\zeta}{\partial r})^2\right]$, where r is the radial coordinate [11, 12]. The critical value depends on the equation of state at the time and the shape of the comoving curvature spectrum. According to simulations, the threshold lies between $0.40 \leq \mathcal{C}_\mathrm{th} \leq \frac{2}{3}$, the lower corresponding to broader spectra and higher to more peaked spectra [1]. The formed PBHs have a mass equal to a fraction $\gamma \approx 0.2$ of

the mass inside the Hubble radius at PBH formation [13]:

$$M_{\mathrm{PBH},*} = \gamma \frac{4\pi}{3} \frac{\rho_*}{H_*^3} = \frac{4\pi\gamma M_{\mathrm{Pl}}^2}{H_*} \ , \tag{2.4}$$

where ρ is the energy density, H is the Hubble parameter, $M_{\mathrm{Pl}} = \frac{1}{\sqrt{8\pi G_n}}$ is the Planck mass, and $*$ denotes a quantity evaluated at the time of the PBH's formation. Since the Hubble radius grows after inflation, PBHs of the same mass are generated at the same time, and smaller ones will form earlier. We can connect the PBH mass to the wavenumber k of the density fluctuation. The mass inside the Hubble radius at matter-radiation equality is

$$M_{\mathrm{eq}} = \frac{4\pi}{3} \frac{2\rho_{\mathrm{r,eq}}}{H_{\mathrm{eq}}^3} \simeq 3.6 \times 10^{17} M_\odot \ , \tag{2.5}$$

so we have

$$\frac{M_{\mathrm{PBH},*}}{M_{\mathrm{eq}}} = \frac{\gamma\rho_*}{2\rho_{\mathrm{r,eq}}} \left(\frac{H_{\mathrm{eq}}}{H_*}\right)^3 \ . \tag{2.6}$$

Now using $k = aH$, the fact that the energy density of radiation decays as $\rho_{\mathrm{r}} \propto a^{-4}$ and the conservation of entropy $g_{*s}a^3T^3 = \mathrm{const}$, where g_{*s} is the number of entropy effective degrees of freedom and T is the temperature we get:

$$M_{\mathrm{PBH},*} = \frac{\gamma}{\sqrt{2}} M_{\mathrm{eq}} \left(\frac{g}{g_{\mathrm{eq}}}\right)^{-\frac{1}{3}} \left(\frac{k}{k_{\mathrm{eq}}}\right)^{-2} \approx 20\gamma M_\odot \left(\frac{k}{10^6\ \mathrm{Mpc}^{-1}}\right)^{-2} \ , \tag{2.7}$$

where $M_\odot$ is the solar mass [14]. This allows us to connect the frequency of the gravitational waves to the mass of the PBH.

2.2 Constraints on primordial black holes

Since there have been no observations of a PBH, we can place bounds on their number density for different masses. In figure 2.1 we show the current constraints on PBH abundance.

Since small PBHs decay quickly to Hawking radiation we can rule out masses under 10^{15} g, which would have already evaporated. The constraints are further strengthened since slightly more massive PBHs would cause a noticeable γ-ray background. We also have constraints from observations of white dwarfs and ultra-faint dwarf galaxies. A large abundance of massive PBHs could heat up white dwarfs triggering supernova explosions [15], and dynamical friction could cause ultra-faint dwarf galaxies to merge with neighboring galaxies [16]. However, the robustness of these constraints is still uncertain, and they should be taken with a grain of salt. A significant amount of PBHs would also cause more gravitational lensing than is currently observed. The relatively small masses involved cause microlensing or nanolensing, which distort objects behind them. These effects are

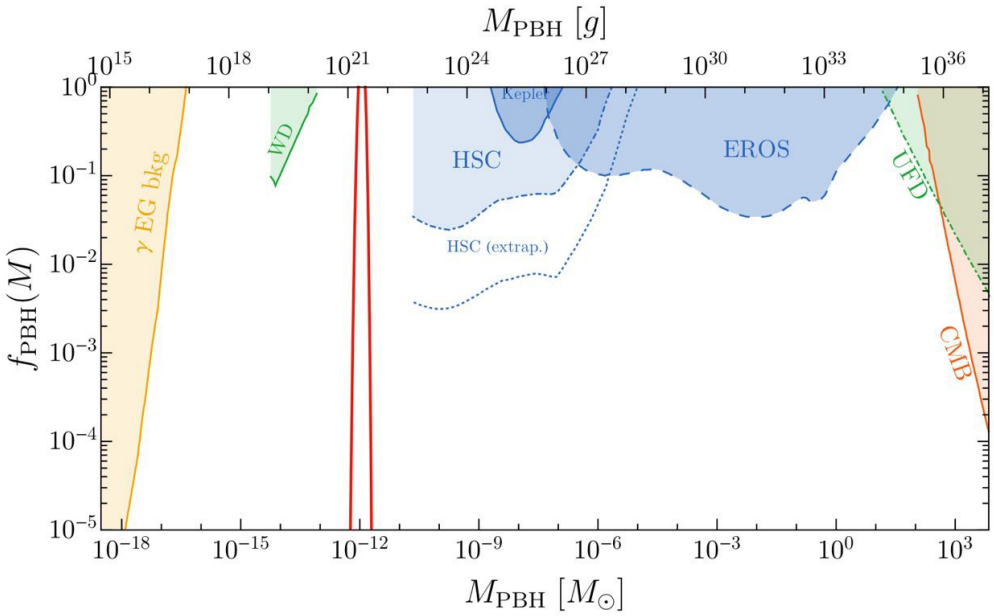

Figure 2.1: The portion of dark matter in PBHs compared with the mass of the PBH from [18]. In yellow are constraints from extra galactic gamma rays, in green the uncertain dynamical heating constraints from white dwarfs and ultra-faint dwarf galaxies, in blue the gravitational lensing constraints, and in orange the CMB constraints. The red line denotes the PBH distribution for a situation where all of dark matter consists of PBHs for a delta-function spectrum with amplitude $A_s = 0.033$ and peak wavenumber $k_p = 2\pi f_p$, $f_p = 3.4$ mHz.

not noticeable by eye but only through statistics. The Subaru HSC microlensing observations are cut around $10^{-11}\ M_\odot$, since below that the geometrical optics approximation doesn't apply. Finally, we have constraints from the CMB. As PBHs accrete matter, some of it is converted to radiation, which would distort the frequency spectrum of the CMB [17].

We can see that between $10^{-17} M_\odot$ and $10^{-11} M_\odot$, which is called the asteroid mass gap, there are currently no well established constraints. The red line shows the mass distribution of PBHs for a model of comoving curvature perturbations enhanced on a single scale k_p if all of dark matter consists of PBHs. Here we used the k_p, which corresponds to the peak sensitivity of LISA and PBHs of mass around $10^{-12}\ M_\odot$.

3. Induced gravitational waves

The density fluctuations generate gravitational waves, which are called induced gravitational waves (iGWs). In this chapter, we derive the equation of motion of the iGWs and find its solutions, mostly following reference [9], and find the energy density of iGWs.

3.1 Equation of motion

The iGWs are described by the second-order tensor perturbation $h_{ij}^{(2)}$ which is sourced by the terms that are quadratic in the first-order scalar perturbations, hence the name scalar-induced gravitational waves. From the metric (2.2), we can find the spatial components of the second-order Einstein tensor [19]

$$\begin{aligned} G^{(2)i}{}_{j} =& a^{-2}\left[\frac{1}{4}(h^{i}{}_{j}{}'' + 2\mathcal{H}h^{i}{}_{j}{}' - 2\nabla^2 h^{i}{}_{j}) + 2\Phi\partial^i\partial_j\Phi - 2\Psi\partial^i\partial_j\Phi\right. \\ &+4\Psi\partial^i\partial_j\Psi + \partial^i\Phi\partial_j\Phi - \partial^i\Phi\partial_j\Psi - \partial^i\Psi\partial_j\Phi + 3\partial^i\Psi\partial_j\Psi \\ &\left.+(\text{diagonal terms})\delta^i_j\right] , \end{aligned} \tag{3.1}$$

where $\mathcal{H} = \frac{a'}{a}$. Now with the energy-momentum tensor, and using the spatial part of the second-order Einstein equation we find an equation of motion for h_{ij}. The spatial components of the energy-momentum tensor are [19]

$$T^{(2)i}{}_{j} = \left(\rho^{(0)} + P^{(0)}\right) v^{i(1)} v_j^{(1)} + P^{(0)}\Pi^{(2)i}{}_{j} + P^{(1)}\Pi^{(1)i}{}_{j} + P^{(2)}\delta^i_j \ , \tag{3.2}$$

where P is the pressure, v_i is the velocity and $\Pi^i{}_j$ is the anisotropic stress. Next we use the Einstein equation with zero cosmological constant:

$$G^{(n)}_{\alpha\beta} = 8\pi G_N T^{(n)}_{\alpha\beta} \ . \tag{3.3}$$

From the background equation $n = 0$ we get the Friedmann equations, the first of which is $\mathcal{H}^2 = \frac{8\pi G_N a^2 \rho^{(0)}}{3}$. The first order equations give us the relations

$$P^{(1)} = c_s^2 \rho^{(1)} \tag{3.4}$$

$$\rho^{(1)} = -\frac{2}{8\pi G_N a^2}[3\mathcal{H}(\mathcal{H}\Phi - \Psi') + \nabla^2\Psi] \tag{3.5}$$

$$v_i^{(1)} = -\frac{2}{8\pi G_N a^2(\rho^{(0)} + P^{(0)})}\partial_i(\Psi' + \mathcal{H}\Phi) \tag{3.6}$$

$$\Pi^{(1)i}{}_j = -\frac{1}{8\pi G_N a^2 P^{(0)}}\partial^i\partial_j(\Phi - \Psi) \ , \tag{3.7}$$

where c_s is the sound speed. Now we can act on the spatial components of the second order Einstein equation with $\hat{\mathcal{T}}_{ij}{}^{lm}$, which projects the transverse traceless part of both tensors [9]

$$\hat{\mathcal{T}}_{ij}{}^{lm} G^{(2)}_{lm} = 8\pi G_N \hat{\mathcal{T}}_{ij}{}^{lm} T^{(2)}_{lm} \ . \tag{3.8}$$

Using the relations (3.4)–(3.7), the second-order Einstein equation (3.8) becomes:

$$\begin{aligned} a^{-2}\hat{\mathcal{T}}_{ij}{}^{lm} \Big[\frac{1}{4}\left(h''_{lm} + 2\mathcal{H}h'_{lm} - \nabla^2 h_{lm}\right) + 2\Phi\partial^l\partial_m\Phi - 2\Psi\partial^l\partial_m\Phi + 4\Psi\partial^l\partial_m\Psi + \partial^l\Phi\partial_m\Phi - \partial^l\Phi\partial_m\Psi \\ -\partial^l\Psi\partial_m\Phi + 3\partial^l\Psi\partial_m\Psi\Big] = 8\pi G_N \hat{\mathcal{T}}_{ij}{}^{lm} \Bigg[\frac{4}{(8\pi G_N)^2 a^4(\rho^{(0)} + P^{(0)})}\partial_l(\Psi' + \mathcal{H}\Phi)\partial_m(\Psi' + \mathcal{H}\Phi) \\ + \frac{2c_s^2}{(8\pi G_N)^2 a^4 P^{(0)}}\left(3\mathcal{H}(\mathcal{H}\Phi - \Psi') + \nabla^2\Psi\right)\partial_l\partial_m(\Phi - \Psi)\Bigg] \ , \end{aligned} \tag{3.9}$$

where we have dropped the tensor part of $\Pi^{(2)i}{}_j$. Using the first Friedmann equation and the equation of state we get the equation of motion for the second order tensor perturbation

$$h''_{ij} + 2\mathcal{H}h'_{ij} - \nabla^2 h_{ij} = -4\hat{\mathcal{T}}_{ij}{}^{lm} S_{lm} \ , \tag{3.10}$$

where:

$$\begin{aligned} S_{ij} = {} & 2\Phi\partial^i\partial_j\Phi - 2\Psi\partial^i\partial_j\Phi + 4\Psi\partial^i\partial_j\Psi + \partial^i\Phi\partial_j\Phi - \partial^i\Phi\partial_j\Psi - \partial^i\Psi\partial_j\Phi + 3\partial^i\Psi\partial_j\Psi \\ & - \frac{4}{3(1+w)\mathcal{H}^2}\partial_i(\Psi' + \mathcal{H}\Phi)\partial_j(\Psi' + \mathcal{H}\Phi) - \frac{2c_s^2}{3w\mathcal{H}^2}[3\mathcal{H}(\mathcal{H}\Phi - \Psi') + \nabla^2\Psi]\partial_i\partial_j(\Phi - \Psi) \ , \end{aligned} \tag{3.11}$$

and $w \equiv \frac{P^{(0)}}{\rho^{(0)}}$ is the equation of state. We can now simplify this by moving away from the general case and neglecting the anisotropic stress from the free-streaming of neutrinos, so $\Phi = \Psi$ [20]. Then, assuming radiation domination (RD) where $w = c_s^2 = \frac{1}{3}$ the source term simplifies to:

$$S_{ij} = 4\Psi\partial^i\partial_j\Psi + 2\partial^i\partial_j\Psi - \frac{1}{\mathcal{H}^2}\partial_i(\Psi' + \mathcal{H}\Psi)\partial_j(\Psi' + \mathcal{H}\Psi) \ . \tag{3.12}$$

It is convenient to write h_{ij} in terms of Fourier modes and use Green's method to find its solutions from the equation of motion. The Fourier transform of the tensor perturbation is:

$$h_{ij}(\mathbf{x},\eta) = \frac{1}{(2\pi)^3}\int \mathrm{d}^3\mathbf{k} e^{i\mathbf{k}\cdot\mathbf{x}}[h_{\mathbf{k}}^{(+)}(\eta)e_{ij}^{(+)}(\mathbf{k}) + h_{\mathbf{k}}^{(\times)}e_{ij}^{(\times)}(\mathbf{k})] \,, \tag{3.13}$$

where $h_{\mathbf{k}}^{(p)}$ is the amplitude of the gravitational waves, $p = +, \times$ is the polarization and $e_{ij}^{(+)}$ and $e_{ij}^{(\times)}$ are polarization tensors defined as

$$e_{ij}^{(+)}(\mathbf{k}) \equiv \frac{1}{\sqrt{2}}[e_i(\mathbf{k})e_j(\mathbf{k}) - \bar{e}_i(\mathbf{k})\bar{e}_j(\mathbf{k})] \tag{3.14}$$

$$e_{ij}^{(\times)}(\mathbf{k}) \equiv \frac{1}{\sqrt{2}}[e_i(\mathbf{k})\bar{e}_j(\mathbf{k}) + \bar{e}_i(\mathbf{k})e_j(\mathbf{k})] \,. \tag{3.15}$$

Here, e_i and $\bar{e}_i$ are normalized vectors that are orthogonal to $\mathbf{k}$, so the polarization tensors satisfy $e^{(p_1)ij}e_{ij}^{(p_2)} = \delta_{p_1,p_2}$. Now in Fourier space equation (3.10) is [21]:

$$h_{\mathbf{k}}^{(p)\prime\prime} + 2\mathcal{H}h_{\mathbf{k}}^{(p)\prime} + k^2 h_{\mathbf{k}}^{(p)} = \hat{\mathcal{S}}^{(p)}(\mathbf{k},\eta) \,, \tag{3.16}$$

and the source term is

$$\begin{aligned}\hat{\mathcal{S}}^{(p)}(\mathbf{k},\eta) = 4\int \frac{\mathrm{d}^3\tilde{\mathbf{k}}}{(2\pi)^3} e^{(p)ij}(\mathbf{k}) \Big[2\hat{\Psi}(\mathbf{k}-\tilde{\mathbf{k}},\eta)\hat{\Psi}(\tilde{\mathbf{k}},\eta) + \left(\hat{\Psi}(\tilde{\mathbf{k}},\eta) + \frac{1}{\mathcal{H}}\hat{\Psi}'(\tilde{\mathbf{k}},\eta)\right) \\ \left(\hat{\Psi}(\mathbf{k}-\tilde{\mathbf{k}},\eta) + \frac{1}{\mathcal{H}}\hat{\Psi}'(\mathbf{k}-\tilde{\mathbf{k}},\eta)\right)\tilde{k}_i\tilde{k}_j\Big] \,.\end{aligned} \tag{3.17}$$

In the last step we introduced the Fourier transform of the scalar perturbation:

$$\hat{\Psi}(\mathbf{k},\eta) = \int \mathrm{d}^3x \Psi(\eta,x)e^{-i\mathbf{k}\cdot x} \,. \tag{3.18}$$

We can now write $\hat{\Psi}$ in terms of the comoving curvature perturbation ζ [22]:

$$\hat{\Psi}(\mathbf{k},\eta) = \frac{2}{3}T(k,\eta)\zeta(\mathbf{k}) \,, \tag{3.19}$$

where $T(k,\eta)$ is the transfer function that tells us how the fluctuations evolve after inflation. During the radiation dominated era $T(k,\eta)$ is [21]:

$$T(k,\eta) = \frac{9}{(k\eta)^2}\left[\frac{\sin(k\eta/\sqrt{3})}{k\eta/\sqrt{3}} - \cos(k\eta/\sqrt{3})\right] . \tag{3.20}$$

Applying the Green's function method we find the solution to (3.16):

$$h_{\mathbf{k}}^{(p)}(\eta) = \frac{1}{a(\eta)}\int \mathrm{d}\tilde{\eta} a(\tilde{\eta})G_{\mathbf{k}}(\eta,\tilde{\eta})\hat{\mathcal{S}}^{(p)}(\mathbf{k},\tilde{\eta}) \,, \tag{3.21}$$

where G_k is the Green's function [21]:

$$G_k(\eta,\tilde{\eta}) = \frac{4}{\pi^2 k}[\sin(k\eta)\cos(k\tilde{\eta}) - \cos(k\eta)\sin(k\tilde{\eta})] \,. \tag{3.22}$$

With (3.19) we can write (3.21) in terms of the comoving curvature perturbation. Using the fact that during RD $a(\eta) \propto \eta$, and defining

$$e^p(\mathbf{k}, \tilde{\mathbf{k}}) \equiv e^{p,ij}(\mathbf{k})\tilde{k}_i\tilde{k}_j = \begin{cases} \frac{1}{\sqrt{2}}\tilde{k}^2 \sin^2\theta \cos 2\phi & \text{if } p = (+) \\ \frac{1}{\sqrt{2}}\tilde{k}^2 \sin^2\theta \sin 2\phi & \text{if } p = (\times) \end{cases}, \tag{3.23}$$

where $\tilde{k}, \theta, \phi$ are the spherical coordinates of $\tilde{\mathbf{k}}$, and

$$f(k_1, k_2, \eta) \equiv 4\left[2T(\eta, k_1)T(\eta, k_2) + \left(T(\eta, k_1) + \frac{1}{\mathcal{H}}T'(\eta, k_1)\right)\left(T(\eta, k_2) + \frac{1}{\mathcal{H}}T'(\eta, k_2)\right)\right], \tag{3.24}$$

we get:

$$\begin{aligned} h^p_{\mathbf{k}}(\eta) =& \frac{4}{9}\int \frac{\mathrm{d}^3\tilde{\mathbf{k}}}{(2\pi)^3}\frac{1}{k^3\eta}e^p(\mathbf{k}, \tilde{\mathbf{k}})\zeta(\tilde{\mathbf{k}})\zeta(\mathbf{k} - \tilde{\mathbf{k}}) \\ & \left[\int^\eta \mathrm{d}\tilde{\eta}\; k(k\tilde{\eta})\left\{\sin(k\eta)\cos(k\tilde{\eta}) - \cos(k\eta)\sin(k\tilde{\eta})\right\} f(\tilde{k}, |\mathbf{k} - \tilde{\mathbf{k}}|, \tilde{\eta})\right] . \end{aligned} \tag{3.25}$$

3.2 Power spectrum of induced gravitational waves

Now we can find the power spectrum of the iGWs P_h, which is defined by [20]:

$$\langle h^{(p)}_{\mathbf{k}}(\eta) h^{(p)}_{\tilde{\mathbf{k}}}(\eta)\rangle = (2\pi)^3\delta(\mathbf{k} + \tilde{\mathbf{k}})\delta_{+\times}\frac{2\pi^2}{k^3}P_h(k, \eta) . \tag{3.26}$$

We can calculate P_h from (3.26) by substituting in the solution to $h_{\mathbf{k}}$ (3.25), and calculating the two point function. After some algebra, we get P_h in terms of the comoving curvature power spectrum $P_\zeta(k)$ [23]:

$$\begin{aligned} P_h(k, \eta) =& \frac{4}{81}\frac{1}{k^2\eta^2}\iint_{\mathscr{S}} \mathrm{d}x\mathrm{d}y\frac{x^2}{y^2}\left[1 - \frac{(1 + x^2 - y^2)^2}{4x^2}\right]^2 P_\zeta(kx)P_\zeta(ky) \\ & \left[\cos^2(k\eta)\mathcal{I}_c^2 + \sin^2(k\eta)\mathcal{I}_s^2 + \sin(2k\eta)\mathcal{I}_c\mathcal{I}_s\right] , \end{aligned} \tag{3.27}$$

where $P_\zeta(k)$ is defined the same way as the iGW power spectrum

$$\langle\zeta(\mathbf{k}_1)\zeta(\mathbf{k}_2)\rangle = (2\pi)^3\delta^{(3)}(\mathbf{k}_1 + \mathbf{k}_2)\frac{2\pi^2}{k_1^3}\mathcal{P}_\zeta(k_1) , \tag{3.28}$$

and the functions $\mathcal{I}_s$ and $\mathcal{I}_c$ are:

$$\mathcal{I}_s(x, y) \equiv \int_{\eta_{in}}^\infty \mathrm{d}\tau\; \tau(-\sin\tau)\cdot 4\left\{2T(x\tau)T(y\tau) + [T(x\tau) + x\tau T'(x\tau)]\,[T(y\tau) + y\tau T'(y\tau)]\right\} \tag{3.29}$$

$$\mathcal{I}_s(x, y) \equiv \int_{\eta_{in}}^\infty \mathrm{d}\tau\; \tau(\cos\tau)\cdot 4\left\{2T(x\tau)T(y\tau) + [T(x\tau) + x\tau T'(x\tau)]\,[T(y\tau) + y\tau T'(y\tau)]\right\} , \tag{3.30}$$

and $x \equiv \frac{\tilde{k}}{k}, \quad y \equiv \frac{|\mathbf{k}-\tilde{\mathbf{k}}|}{k}, \quad \tau \equiv k\tilde{\eta}$. The domain $\mathscr{S}$ in (3.27) is defined by the triangle inequality between $\mathbf{k}$, $\tilde{\mathbf{k}}$ and $\mathbf{k}-\tilde{\mathbf{k}}$ shown in [21], and η_{in} is the time at which the wavelength $\frac{1}{k} = H$, and the iGWs start to generate. Using the power spectrum of the gravitational waves, we can find their energy density [24]:

$$\rho_{iGW}(\mathbf{x},\eta) \simeq \frac{M_{Pl}^2}{16a^2(\eta)} \left\langle \overline{(\nabla h_{ij})^2} \right\rangle \ , \tag{3.31}$$

where overline denotes a time average over the oscillating terms. In terms of P_h, the energy density is:

$$\rho_{iGW}(k,\eta) = \frac{M_{Pl}^2}{8} \left(\frac{k}{a(\eta)}\right)^2 \overline{P_h(k,\eta)} \ . \tag{3.32}$$

Now we can define the density parameter of the iGWs:

$$\Omega_{iGW}(k,\eta) \equiv \frac{\rho_{iGW}(k,\eta)}{\rho_c(\eta)} \ , \tag{3.33}$$

where $\rho_c \equiv \frac{3H^2}{M_{Pl}^2}$ is the critical density and $H = \frac{\mathcal{H}}{a(\eta)}$. Inserting ρ_c, the density parameter becomes:

$$\Omega_{iGW}(k,\eta) = \frac{1}{24} \left(\frac{k}{\mathcal{H}}\right)^2 \overline{P_h(k,\eta)} \ . \tag{3.34}$$

Equation (3.27) gives the power spectrum during RD so (3.34) works then, but during matter domination, the iGW density parameter starts to decay because the critical density now scales as $\rho_c \propto a^{-3}$ while the energy density of iGWs continues to scale as $\rho_{iGW} \propto a^{-4}$. The energy density of iGWs today is

$$\rho_{iGW,0} = \frac{a_f^4 \rho_{iGW,f}}{a_0^4} \ , \tag{3.35}$$

where the subscripts f and 0 denote a time during RD and the present time. Now we can use the definition of the density parameter (3.33), and that during RD $\rho_{r,f} \approx \rho_{c,f}$, to find the density parameter today:

$$\Omega_{iGW}(k,\eta_0) = c_g \frac{\Omega_{r,0}}{24} \frac{k^2}{\mathcal{H}(\eta_f)^2} \overline{\mathcal{P}_h(k,\eta_f)}, \tag{3.36}$$

where $c_g \equiv \frac{a_f^4 \rho_{r,f}}{a_0^4 \rho_{r,0}}$. The radiation energy densities can be linked to the degrees of freedom, so using the conservation of entropy, we find $c_g \approx 0.4$. Then we can insert (3.27) and find [23]

$$\begin{aligned} \Omega_{iGW}(k,\eta_0) =& \frac{c_g \Omega_{r,0}}{72} \int_{-\frac{1}{\sqrt{3}}}^{\frac{1}{\sqrt{3}}} \mathrm{d}d \int_{\frac{1}{\sqrt{3}}}^{\infty} \mathrm{d}s \frac{x^2}{y^2} \left[\frac{\left(d^2-\frac{1}{3}\right)\left(s^2-\frac{1}{3}\right)}{s^2-d^2}\right]^2 \mathcal{P}_\zeta\left(\frac{k\sqrt{3}}{2}(s+d)\right) \\ & \times \mathcal{P}_\zeta\left(\frac{k\sqrt{3}}{2}(s-d)\right) \mathcal{I}^2 \ , \end{aligned} \tag{3.37}$$

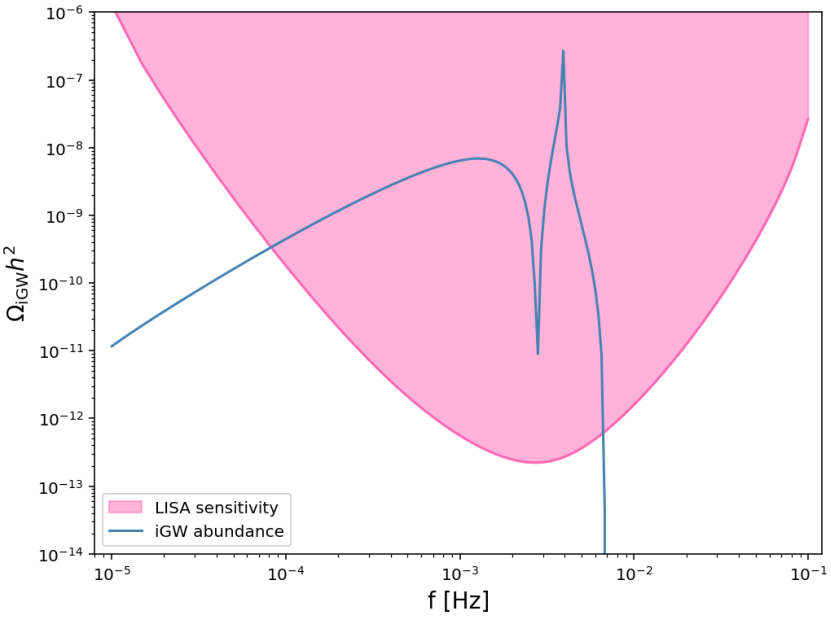

Figure 3.1: The energy density parameter of the iGWs for a monochromatic comoving curvature power spectrum (3.39) with $A_s = 0.033$, $f_p = 3.4$ mHz compared with an expectation of LISA sensitivity from [25] for the approved design [26].

where $\mathcal{I}^2 = \mathcal{I}_c^2 + \mathcal{I}_s^2$, the new integration variables are $d = (x-y)/\sqrt{3}$ and $s = (x+y)/\sqrt{3}$, and we used $\overline{\cos^2(k\eta)} = \overline{\sin^2(k\eta)} = \frac{1}{2}$ when $k\eta \gg 1$ to simplify the time average. We can now calculate the density parameter for a given comoving curvature power spectrum. To generate PBHs, the power spectrum must have a large amplitude. While the power spectrum retains its shape on large scales, on the smaller scales, we assume a delta function case, which corresponds to large fluctuations on a single scale k_p:

$$\mathcal{P}_\zeta(k) = A_s k_p \delta(k - k_p) \ , \tag{3.38}$$

where A_s is the spectrum amplitude. This is not possible for real inflation models [27], but allows the calculations to be done analytically and gives a good approximation of the energy density. Inserting (3.38) into (3.37) we get:

$$\Omega_{\mathrm{iGW}}(k, \eta_0) = \frac{c_g}{15552} \Omega_{r,0} A_s^2 \frac{k^2}{k_p^2} \left(\frac{4k_p^2}{k^2} - 1 \right)^2 \mathcal{I}^2(\frac{k_p}{k}, \frac{k_p}{k}) \theta(2k_p - k) \ , \tag{3.39}$$

where θ is the Heaviside step function. We show this in figure (3.1) for $k_p = 2\pi f_p$, $f_p = 3.4$ mHz which corresponds to a PBH of mass $\sim 10^{-12}\ M_\odot$ by (2.7). The approximation of a monochromatic power spectrum gives the correct amplitude, but has the unphysical features of a slow drop off at low frequencies and a sharp peak at $f = \frac{2f_p}{\sqrt{3}}$ [18]. A more realistic spectrum would have a smoother, but still pronounced peak for a narrow mass range of PBHs. We see that the gravitational waves corresponding to a significant amount of asteroid mass black holes would be detected by LISA.

4. Detection with LISA

LISA is an upcoming gravitational wave detector by ESA in collaboration with NASA planned to launch in 2035. It consists of 3 satellites approximately 2.5 million kilometers apart from each other in the shape of an equilateral triangle that orbit the sun behind the Earth. LISA works by measuring distance changes on scales of pm to nm between test masses in the satellites using interferometry [26]. In this chapter, we will go over whether LISA can detect the iGWs, what it observes, and briefly other detectors.

4.1 Sensitivity

LISA's sensitivity window is between 0.1 mHz and 0.1 Hz [28]. Using (2.7) with $k = 2\pi f$, where f is the frequency, the range corresponds to probing PBH masses between $10^{-15}M_\odot$ and $10^{-8}M_\odot$, which covers most of the asteroid mass gap. Figure (3.1) shows the sensitivity of LISA for the approved design compared to the energy density spectrum of iGWs. The figure shows that a comoving curvature spectrum amplified at a peak scale corresponding to the peak frequency of LISA would generate detectable GWs. For a different peak frequency the iGW abundance would shift right for a larger value or left for a smaller one, but still remain detectable for 10^{-5} Hz $< f_\mathrm{p} <$ 0.5 Hz. The sensitivity expectation uses the detection threshold signal to noise ratio of 10, and the full planned operation time of 4.5 years. However, reaching a similar sensitivity is possible in only a month if the noise from the galactic foreground can be subtracted [29].

4.2 The observable

LISA and other gravitational wave detectors measure the strain h of gravitational waves, which means how much they distort spacetime. The iGWs are in superposition coming from all directions, so we can't resolve the signal of a single source. Therefore, the power spectral density (PSD) of the iGW background's Fourier modes S_h is used. The PSD of the Fourier modes is defined such that the mean square fluctuation of the strain is $\langle h^2 \rangle = \int S_h(f)\ \mathrm{d}f$. The energy density of the gravitational waves is related to the PSD

by [30]:

$$\Omega_{\text{iGW}} = \frac{2\pi^2}{3H_0^2} f^3 S_h(f) \ . \tag{4.1}$$

The measurement of a stochastic GW signal in a single detector is indistinguishable from noise, which means we need more than one detector [31]. The three spacecraft of LISA form two independent detectors, and the stochastic signal will be correlated between the two. The quantities Ω_{iGW} and S_h depend only on the iGW background, and are independent of the detector. The measured quantity however is not the PSD of the Fourier modes, but the PSD of the strain signal S_s which depends on the geometry of the detector. To compare observations with theoretical predictions, we should use the detector independent quantity S_h, which is found by using the overlap reduction function [30]:

$$S_h = \frac{5 S_s}{\sin^2 \beta} \ , \tag{4.2}$$

where $\beta = 60°$ is the angle between the arms.

4.3 Other detectors

It is also possible that the GW signal will be observed before the launch of LISA, as a Chinese GW detector Taiji is expected to launch in 2033. Taiji is very similar to LISA in concept, but with a slightly longer arm length of 3 million km. Its planned sensitivity covers the same range as LISA, but it will be slightly better between 0.01 Hz and 0.1 Hz [32]. Another Chinese detector TianQin is proposed to launch around the same time as LISA. TianQin is a smaller space-based detector in a geocentric orbit, which will be sensitive to slightly higher frequencies than LISA and Taiji, between 0.1 mHz and 1 Hz [33]. Multiple detectors will also lead to a better sensitivity, as you can compare the signals, and the instrument noise will average to zero [29].

5. Conclusions

The comoving curvature power spectrum describes the density fluctuations that on large scales later form galaxies and other structures. The fluctuations have a very small amplitude on cosmic scales, but if the comoving curvature power spectrum is enhanced strongly enough on small scales, some fluctuations will collapse into PBHs. These PBHs can form over a large range of masses, but PBHs as a significant fraction of dark matter is ruled out for most of them. The exception is the asteroid mass gap $M \in [10^{-17}M_{\odot}, 10^{-11}M\odot]$, where PBHs could form all or most of dark matter.

The fluctuations with smaller amplitudes generate a stochastic gravitational wave background. The frequency of the GWs is inversely proportional to the mass of the PBHs, which for asteroid mass PBHs is near LISA's peak sensitivity. For a monochromatic enhancement of the comoving curvature power spectrum, the GW signal is detectable by LISA. For other spectra, the shape of the signal changes, but the result is the same.

If no detection happens, we can rule out PBHs as a significant part of dark matter, but if we do detect GWs, PBHs are not necessarily a large part of dark matter. This is because the fraction of PBH dark matter f_{PBH} depends exponentially on the amplitude of the perturbations, so a small decrease in A_s will lead to a large change in f_{PBH}, but a similar GW signal. This allows us to detect the iGW signal even if $f_{\mathrm{PBH}} \ll 1$. In fact, since the iGW signal is so far inside LISA's sensitivity range, the signal would only become undetectable after reducing A_s by a factor of 100 [18]. Regardless of the result, LISA will enable a new way of studying the early universe, and we are bound to learn something new.

Bibliography

[1] Anne M. Green and Bradley J. Kavanagh. "Primordial Black Holes as a dark matter candidate". In: *J. Phys. G* 48.4 (2021), p. 043001. DOI: 10.1088/1361-6471/abc534. arXiv: 2007.10722 [astro-ph.CO].

[2] Daniel Baumann. "Inflation". In: *Theoretical Advanced Study Institute in Elementary Particle Physics: Physics of the Large and the Small*. 2011, pp. 523–686. DOI: 10.1142/9789814327183_0010. arXiv: 0907.5424 [hep-th].

[3] N. Aghanim et al. "Planck 2013 results. XXVII. Doppler boosting of the CMB: Eppur si muove". In: *Astron. Astrophys.* 571 (2014), A27. DOI: 10.1051/0004-6361/201321556. arXiv: 1303.5087 [astro-ph.CO].

[4] Gianfranco Bertone and Dan Hooper. "History of dark matter". In: *Rev. Mod. Phys.* 90.4 (2018), p. 045002. DOI: 10.1103/RevModPhys.90.045002. arXiv: 1605.04909 [astro-ph.CO].

[5] Marek Szczepańczyk et al. "Observing an intermediate-mass black hole GW190521 with minimal assumptions". In: *Phys. Rev. D* 103.8 (2021), p. 082002. DOI: 10.1103/PhysRevD.103.082002. arXiv: 2009.11336 [astro-ph.HE].

[6] Alberto Magaraggia and Nico Cappelluti. "Implications for Primordial Black Hole Dark Matter from a Single Subsolar Mass Gravitational-wave Detection in LVK O1–O4". In: *Astrophys. J.* 1000.2 (2026), p. 262. DOI: 10.3847/1538-4357/ae48f9. arXiv: 2602.21295 [astro-ph.CO].

[7] Rebecca L. et al. Larson. "A CEERS Discovery of an Accreting Supermassive Black Hole 570 Myr after the Big Bang: Identifying a Progenitor of Massive z gt; 6 Quasars". In: *The Astrophysical Journal Letters* 953.2 (Aug. 2023), p. L29. ISSN: 2041-8213. DOI: 10.3847/2041-8213/ace619. URL: http://dx.doi.org/10.3847/2041-8213/ace619.

[8] J. Aasi et al. "Advanced LIGO". In: *Class. Quant. Grav.* 32 (2015), p. 074001. DOI: 10.1088/0264-9381/32/7/074001. arXiv: 1411.4547 [gr-qc].

[9] Daniel Baumann et al. "Gravitational Wave Spectrum Induced by Primordial Scalar Perturbations". In: *Phys. Rev. D* 76 (2007), p. 084019. DOI: 10.1103/PhysRevD.76.084019. arXiv: hep-th/0703290.

[10] Hannu Kurki-Suonio. "Cosmological Perturbation Theory I". In: *Lecture notes* (2024).

[11] Tomohiro Harada, Chul-Moon Yoo, and Yasutaka Koga. "Revisiting compaction functions for primordial black hole formation". In: *Phys. Rev. D* 108.4 (2023), p. 043515. DOI: 10.1103/PhysRevD.108.043515. arXiv: 2304.13284 [gr-qc].

[12] Sami Raatikainen, Syksy Rasanen, and Eemeli Tomberg. "Effect of stochastic kicks on primordial black hole abundance and mass via the compaction function". In: *JCAP* 03 (2026), p. 063. DOI: 10.1088/1475-7516/2026/03/063. arXiv: 2510.09303 [astro-ph.CO].

[13] Guillem Domènech. "Scalar Induced Gravitational Waves Review". In: *Universe* 7.11 (2021), p. 398. DOI: 10.3390/universe7110398. arXiv: 2109.01398 [gr-qc].

[14] Juan Garcia-Bellido, Marco Peloso, and Caner Unal. "Gravitational Wave signatures of inflationary models from Primordial Black Hole Dark Matter". In: *JCAP* 09 (2017), p. 013. DOI: 10.1088/1475-7516/2017/09/013. arXiv: 1707.02441 [astro-ph.CO].

[15] Peter W. Graham, Surjeet Rajendran, and Jaime Varela. "Dark Matter Triggers of Supernovae". In: *Phys. Rev. D* 92.6 (2015), p. 063007. DOI: 10.1103/PhysRevD.92.063007. arXiv: 1505.04444 [hep-ph].

[16] Timothy D. Brandt. "Constraints on MACHO Dark Matter from Compact Stellar Systems in Ultra-Faint Dwarf Galaxies". In: *Astrophys. J. Lett.* 824.2 (2016), p. L31. DOI: 10.3847/2041-8205/824/2/L31. arXiv: 1605.03665 [astro-ph.GA].

[17] Yacine Ali-Haïmoud and Marc Kamionkowski. "Cosmic microwave background limits on accreting primordial black holes". In: *Phys. Rev. D* 95.4 (2017), p. 043534. DOI: 10.1103/PhysRevD.95.043534. arXiv: 1612.05644 [astro-ph.CO].

[18] N. Bartolo et al. "Primordial Black Hole Dark Matter: LISA Serendipity". In: *Phys. Rev. Lett.* 122.21 (2019), p. 211301. DOI: 10.1103/PhysRevLett.122.211301. arXiv: 1810.12218 [astro-ph.CO].

[19] Viviana Acquaviva et al. "Second order cosmological perturbations from inflation". In: *Nucl. Phys. B* 667 (2003), pp. 119–148. DOI: 10.1016/S0550-3213(03)00550-9. arXiv: astro-ph/0209156.

[20] Kenta Ando et al. "Primordial black holes for the LIGO events in the axionlike curvaton model". In: *Phys. Rev. D* 97.12 (2018), p. 123512. DOI: 10.1103/PhysRevD.97.123512. arXiv: 1711.08956 [astro-ph.CO].

[21] José Ramón Espinosa, Davide Racco, and Antonio Riotto. "A Cosmological Signature of the SM Higgs Instability: Gravitational Waves". In: *JCAP* 09 (2018), p. 012. DOI: 10.1088/1475-7516/2018/09/012. arXiv: 1804.07732 [hep-ph].

[22] David H. Lyth and Antonio Riotto. "Particle physics models of inflation and the cosmological density perturbation". In: *Phys. Rept.* 314 (1999), pp. 1–146. DOI: 10.1016/S0370-1573(98)00128-8. arXiv: hep-ph/9807278.

[23] N. Bartolo et al. "Testing primordial black holes as dark matter with LISA". In: *Phys. Rev. D* 99.10 (2019), p. 103521. DOI: 10.1103/PhysRevD.99.103521. arXiv: 1810.12224 [astro-ph.CO].

[24] Michele Maggiore. "Gravitational wave experiments and early universe cosmology". In: *Phys. Rept.* 331 (2000), pp. 283–367. DOI: 10.1016/S0370-1573(99)00102-7. arXiv: gr-qc/9909001.

[25] Stanislav Babak, Antoine Petiteau, and Martin Hewitson. "LISA Sensitivity and SNR Calculations". In: (Aug. 2021). arXiv: 2108.01167 [astro-ph.IM].

[26] H. Audley et al. *Laser Interferometer Space Antenna*. 2017. arXiv: 1702.00786 [astro-ph.IM]. URL: https://arxiv.org/abs/1702.00786.

[27] Christian T. Byrnes, Philippa S. Cole, and Subodh P. Patil. "Steepest growth of the power spectrum and primordial black holes". In: *JCAP* 06 (2019), p. 028. DOI: 10.1088/1475-7516/2019/06/028. arXiv: 1811.11158 [astro-ph.CO].

[28] B. S. Sathyaprakash and B. F. Schutz. "Physics, Astrophysics and Cosmology with Gravitational Waves". In: *Living Rev. Rel.* 12 (2009), p. 2. DOI: 10.12942/lrr-2009-2. arXiv: 0903.0338 [gr-qc].

[29] Matthew R. Adams and Neil J. Cornish. "Discriminating between a stochastic gravitational wave background and instrument noise". In: *Phys. Rev. D* 82 (2 July 2010), p. 022002. DOI: 10.1103/PhysRevD.82.022002. URL: https://link.aps.org/doi/10.1103/PhysRevD.82.022002.

[30] Chiara M. F. Mingarelli et al. "Understanding $\Omega_{\rm gw}(f)$ in Gravitational Wave Experiments". In: (Nov. 2019). arXiv: 1911.09745 [gr-qc].

[31] Lee Samuel Finn, Shane L. Larson, and Joseph D. Romano. "Detecting a Stochastic Gravitational-Wave Background: The Overlap Reduction Function". In: *Phys. Rev. D* 79 (2009), p. 062003. DOI: 10.1103/PhysRevD.79.062003. arXiv: 0811.3582 [gr-qc].

[32] Yungui Gong, Jun Luo, and Bin Wang. "Concepts and status of Chinese space gravitational wave detection projects". In: *Nature Astron.* 5.9 (2021), pp. 881–889. DOI: 10.1038/s41550-021-01480-3. arXiv: 2109.07442 [astro-ph.IM].

[33] Jun Luo et al. "Progress of the TianQin project". In: *Class. Quant. Grav.* 42.17 (2025), p. 173001. DOI: 10.1088/1361-6382/adda8a. arXiv: 2502.11328 [gr-qc].